Modified Kagome Physics in the Natural Spin-1/2 Kagome Lattice Systems: Kapellasite $Cu_3Zn(OH)_6Cl_2$ and Haydeeite $Cu_3Mg(OH)_6Cl_2$

O. Janson,[1] J. Richter,[2] and H. Rosner[1,*]

[1]*Max-Planck-Institut für Chemische Physik fester Stoffe, D-01187 Dresden, Germany*
[2]*Institut für Theoretische Physik, Universität Magdeburg, D-39016 Magdeburg, Germany*
(Received 26 May 2008; published 3 September 2008)

The recently discovered natural minerals $Cu_3Zn(OH)_6Cl_2$ and $Cu_3Mg(OH)_6Cl_2$ are spin 1/2 systems with an ideal kagome geometry. Based on electronic structure calculations, we develop a realistic model which includes couplings across the kagome hexagons beyond the original kagome model that are intrinsic in real kagome materials. Exact diagonalization studies for the derived model reveal a strong impact of these couplings on the magnetic ground state. Our predictions could be compared to and supplied with neutron scattering, thermodynamic data, and NMR data.

For decades, low-dimensional spin systems have attracted broad interest due to their intriguing, unusual ground states (GS) such as helically ordered, spin Peierls, spin-liquid, or resonating valence-bond GS's [1–4]. These unusual GS's are typically driven by competing interactions or geometric frustration. Two-dimensional (2D) quantum spin systems are of particular interest because the competition between quantum fluctuations and interactions seems to be well balanced, and fine-tuning of this competition may lead to zero-temperature transitions between semiclassical and quantum phases [5]. There are several examples for strongly frustrated 2D quantum spin materials, e.g., $PbVO_3$ [6] or $SrCu_2(BO_3)_2$ [7], which can be well described by a frustrated spin-1/2 Heisenberg model. Such 2D quantum magnets are at present most suitable objects for the comparison between theory and experiment.

A simple but very challenging realization of a geometrically frustrated quantum magnet is the spin-1/2 Heisenberg antiferromagnet (HAFM) on a kagome lattice. The kagome HAFM attracts much interest due to its unusual classical and quantum GS's and low-temperature thermodynamics, see, e.g., Refs. [8–13], and also due to potential applications of a possible quantum spin-liquid state [14,15]. The recent discovery of a natural spin-1/2 kagome compound $Cu_3Zn(OH)_6Cl_2$ (mineral herbertsmithite [16]) and a subsequent synthesis of good-quality samples [17] have spurred both experimental [18,19] and theoretical [11–13] investigations of this frustrated magnetic system. The experimental results were quite unexpected: Curie-Weiss behavior with a rather large Θ, an upturn in magnetic susceptibility at 75 K and no spin gap down to 100 mK are far from being consistently described by theory. The main obstacle for theoretical studies is the structural Cu–Zn disorder within this compound [20], which hampers the kagome physics, but encourages the search for new materials. A very recent discovery of two isostructural spin-1/2 kagome systems—the minerals kapellasite $Cu_3Zn(OH)_6Cl_2$ ([21], a metastable polymorph of

herbertsmithite), and haydeeite $Cu_3Mg(OH)_6Cl_2$ [22]—widens the range of possible investigations. These systems are of great potential interest because (i) no cations are located between the planes, thus less coupling between kagome layers is expected though the interlayer distance is reduced by about 1 Å; (ii) the presence of two isostructural compounds should allow a systematic study of additional exchange couplings beyond the original kagome model. We have performed a theoretical electronic structure study within density functional theory (DFT) and estimated the exchange parameters of a corresponding Heisenberg model. For this spin model, we have calculated the classical GS, and for a finite lattice of $N = 36$ sites, the quantum spin-1/2 GS.

The DFT calculations were performed using a full-potential nonorthogonal local-orbital scheme (FPLO version 6.00-24) [23] within the local density approximation (LDA). The Perdew and Wang parameterization of the exchange-correlation potential was chosen for the scalar relativistic calculations [24]. The default basis set was used. The strong on-site correlations of the Cu d-electrons were taken into account using the LSDA + U method [25]. Well converged k-meshes of 124 points for the conventional cell and 75 points for the supercell in the irreducible wedge were used.

The hexagonal crystal structure of both minerals consists of layers (Fig. 1) perpendicular to the c direction. These layers are built by a kagome lattice of corner-sharing CuO_4 plaquettes, which are tilted with respect to this plane, and ZnO_6 (kapellasite) or MgO_6 (haydeeite) octahedra bridging the "ring" of six CuO_4 plaquettes. The Cu–O–Cu angle between two neighboring plaquettes is close to 105°, providing considerable ferromagnetic (FM) contributions to the exchange due to the vicinity to 90°. The kagome layers are separated by Cl atoms, which are bonded to H atoms that stick out of the layers. The experimentally defined H position for haydeeite [26] yields the unusually short O–H distance of 0.78 Å; the H position in kapellasite has not been reported. To account for this
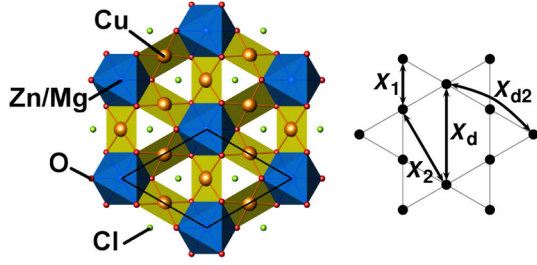
FIG. 1 (color online). The hexagonal crystal structure of ka-pellasite and haydeeite: CuO_4 plaquettes form a buckled kagome layer bridged by ZnO_6/MgO_6 octahedra. The interlayer space is filled with Cl and H (not shown) atoms.

structural peculiarity, the H position was relaxed with respect to the total energy. We show below that it has a dramatic impact on the exchange. Throughout the Letter, we use the optimized H position [27] yielding ~ 1.0 Å for the O–H distance (Fig. 2).

Our LDA calculations yield a valence band with a total width of 6–7 eV for both compounds with three bands crossing the Fermi level ε_F according to the three Cu atoms per unit cell (Fig. 3). The valence bands of haydeeite and kapellasite have two pronounced differences: (1) the rather localized d-states of Zn (between -6.5 and -4 eV) contribute to the valence band of kapellasite while Mg states have negligible contribution for haydeeite, and (2) the width of the separated band complex at ε_F is slightly different. Nevertheless, the same model can be applied for the description of low-energy excitations.

The band structure (Fig. 3) reveals that the dispersion perpendicular to the kagome planes (along Γ–A) is very small, pointing to a pronounced 2D character of the systems in accordance with our expectations. The presence of states at Fermi level yields a metallic GS, contrary to the

insulating behavior typical for undoped cuprates [28]. This discrepancy originates from the strong on-site correlations of the Cu $3d$ electrons, insufficiently described by LDA, and can be accounted for by adding the missing Coulomb repulsion in a model Hamiltonian or in the LSDA $+ U$ approximation. Though LDA fails to describe the correlations correctly, it is known to provide reliable values of transfer integrals [29] which can be used for a model analysis of the magnetic excitations. To define the relevant orbitals for the low-energy excitations, we analyzed the density of states (DOS) by applying local coordinate systems for all orientations of CuO_4 plaquettes and calculated the local DOS and band weights. The analysis revealed that the bands at Fermi level belong to local Cu $3d_{x^2-y^2}$ and O $2p_\sigma$ orbitals; i.e., the standard cuprate scenario with a half-filled antibonding $dp\sigma^*$ band is realized. Therefore, an effective one-band model, already applied for similar materials [30,31], is appropriate to describe the magnetic excitations in these systems.

Three $dp\sigma^*$ bands per unit cell lead to a 3×3 matrix representing the tight-binding (TB) Hamiltonian. The number of transfer integrals, included into the TB model, was picked to get a good fit of the LDA bands which could not be considerably improved by inclusion of further parameters. The fits shown in Fig. 3 were achieved using ten transfer integrals, though only four of them (Fig. 1) were larger than 10 meV. To check the stability of the leading terms, we subsequently decreased the number of parameters in our model. Based on these results, we estimate less than 10% uncertainty in our values for the leading four transfer integrals depending on the chosen TB Hamiltonian. Thus, we can restrict ourselves to analysis of the leading terms. In order to estimate the antiferromagnetic (AF) exchange, the transfer integrals were mapped to an extended Hubbard model and subsequently to a Heisenberg model with $J_i^{AF} = 4t_i^2/U_{eff}$ [32].

The leading AF exchange in both systems is the nearest-neighbor (NN) exchange J_1^{AF}, the second largest is the exchange along diagonals of a kagome lattice, J_d^{AF} (see
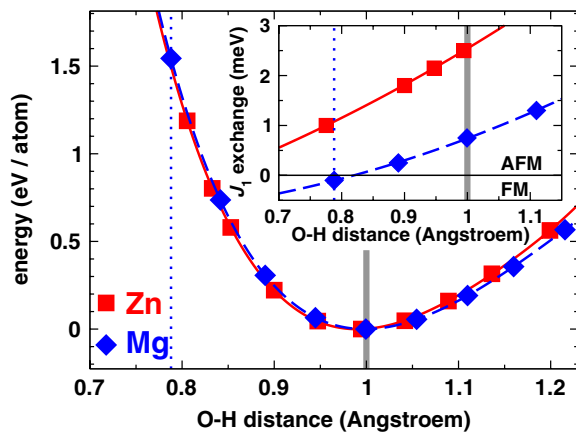

FIG. 2 (color online). Total energy per H atom given by LDA calculations for kapellasite (Zn) and haydeeite (Mg). The zero energy corresponds to the calculated equilibrium distance and is marked with a gray line. The experimental value of the O–H distance in haydeeite is shown with a dotted line. Inset: exchange J_1 from the supercell LSDA $+ U$ calculations as a function of the O–H distance.
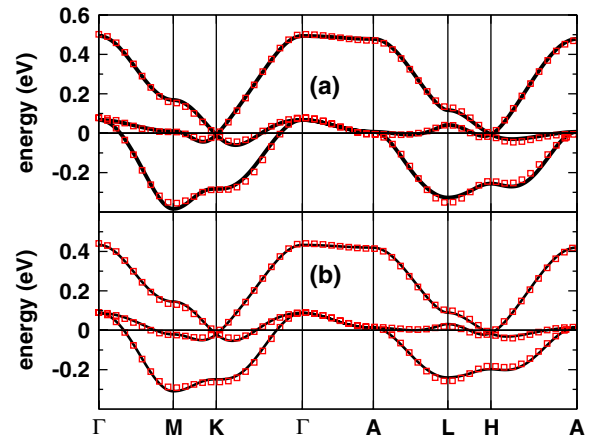

FIG. 3 (color online). TB model (squares) fitted to the band structures (solid lines) of kapellasite (a) and haydeeite (b).

Fig. 1). The relevance of the latter exchange is rather unexpected: while the pure kagome model includes J_1 only, its modifications usually contain only the second neighbor J_2 [33]. In our case, we find J_2^{AF} (and also J_{d2}^{AF}) smaller than 0.5 meV for both systems; thus, these terms can be neglected in the following discussion. The interplane coupling is much smaller than 0.1 meV, showing that the systems are almost perfect 2D magnets. Therefore, a J_1-J_d model should be appropriate to describe the magnetism in good approximation.

The values of the total exchange were obtained using total energy calculations for supercells with different spin arrangements, where the difference in the values of total energy originates only from spin degrees of freedom. To obtain the leading exchange integrals, we used a doubled cell with six Cu atoms. The supercell calculations were performed using the LSDA + U method treating the correlation on a mean field level. This approach is necessary due to the Cu–O–Cu bond angle $\approx 105°$ which leads to sizable FM contribution according to Goodenough-Kanamori-Anderson rules.

The results are given in Table I (J^{FM} was evaluated as the difference between the total J and $J^{AF} = 4t^2/U_{eff}$). The FM contributions significantly modify the size of the relevant exchange integrals, but preserve their AF nature. Here, we introduce the ratio $\alpha \equiv J_d/J_1$, which is zero in the simple kagome model and runs to infinity in case of decoupled chains. Certainly, α may depend on external parameters like the H position and the U values. The change in O–H distance drastically affects the J_1 exchange (Fig. 2, inset) in both compounds, and especially in haydeeite, where it becomes FM when the O–H bond is shorter than 0.8 Å. Thus, further quantitative analysis is based on the empirical fact that total energy calculations provide in general rather precise atomic positions. An accurate experimental determination of the H position is highly desirable for an improvement. The influence of the Coulomb repulsion U on α is much weaker, and there are no drastic changes in verified region (Fig. 4): α is very close to 0.36 for kapellasite and stays in the vicinity of unity for haydeeite for the whole range of U studied. While GS's for

$\alpha = 0$ and $\alpha = \infty$ are relatively clear, the region in between is not studied. Therefore, we have performed exact diagonalization studies in order to clarify the influence α on the GS.

It is well known that the classical GS of the pure kagome HAFM ($\alpha = 0$) is highly degenerate [8–10]. The additional diagonal bond J_d reduces this degeneracy drastically and selects noncoplanar GS's with 12 magnetic sublattices [34] among the huge number of classical kagome GS's. These classical GS's of the J_1-J_d model are characterized by a perfect antiparallel (Néel) spin alignment along the chains formed by diagonal bonds J_d and by a 120° spin arrangement on each triangle formed by NN bonds J_1. As a result, every two spin-sublattices are Néel-like antiparallel to each other, and these two sublattices are perpendicular to one other group of 2 Néel-like sublattices.

For the quantum model, the GS and low-lying excitations have been calculated by Lanczos diagonalization for the finite lattice of $N = 36$ considered previously in the literature for the pure kagome HAFM. Note that this finite lattice fits to the magnetic structure of the classical GS. The calculated spin correlations $\langle \mathbf{S}_0 \mathbf{S}_R \rangle$ for the classical GS as well as for the quantum GS for $\alpha = 0.36$ and $\alpha = 1.0$ are shown in Fig. 5. For comparison, we also show $\langle \mathbf{S}_0 \mathbf{S}_R \rangle$ for the pure kagome system, i.e., $J_d = 0$. Obviously, the quantum GS spin correlation is drastically changed by J_d. While for $J_d = 0$ the decay of the spin correlation function is extremely rapid, we find a well-pronounced short-range order for $\alpha = 0.36$ and $\alpha = 1.0$ that corresponds to the classical magnetic structure. This leads to the conclusion that even in the quantum model, the GS has a noncoplanar magnetic structure giving rise to enhanced chiral correlations. Moreover, it is obvious from Fig. 5 that the magnetic correlations along the chains built by J_d bonds ($R/R_{NN} = 2$ and 4) are strongest, indicating that the low-energy excitations might be $S = 1/2$ spinons causing an effectively one-dimensional low-temperature physics similar to other 2D models, e.g., the crossed-chain model [35] and the anisotropic triangular lattice [36]. However, this issue needs further investigation.

Finally, we mention another important difference from the pure kagome system which is relevant for the low-temperature thermodynamics. For $\alpha = 0$, the singlet-triplet gap (spingap) is filled by 210 nonmagnetic excita-
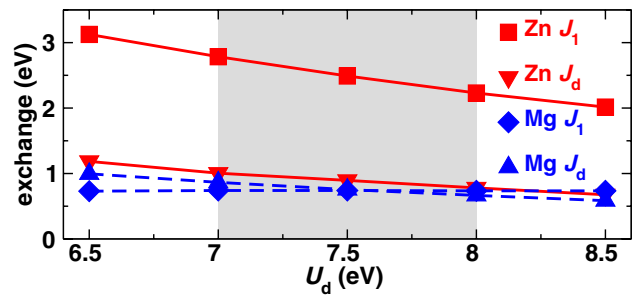
TABLE I. Transfer and exchange integrals of kapellasite and haydeeite. All values are given in meV. The values of transfer integrals are taken from the TB model. The AF exchange is calculated via subsequent mapping of the transfer integrals to the extended Hubbard and Heisenberg models. The total exchange is taken from LSDA + U total energy calculations of supercells. J^{FM} is the difference between J and J^{AF}.

	kapellasite				haydeeite			
path	t	J^{AF}	J^{FM}	J	t	J^{AF}	J^{FM}	J
X_1	87	7.5	−5.0	2.5	73	5.3	−4.5	0.8
X_2	−10	0.1	~0	<0.1	−9	0.1	~0	<0.1
X_d	49	2.4	−1.5	0.9	42	1.8	−1.0	0.8
X_{d2}	20	0.4	−0.4	<0.1	22	0.5	−0.5	<0.1

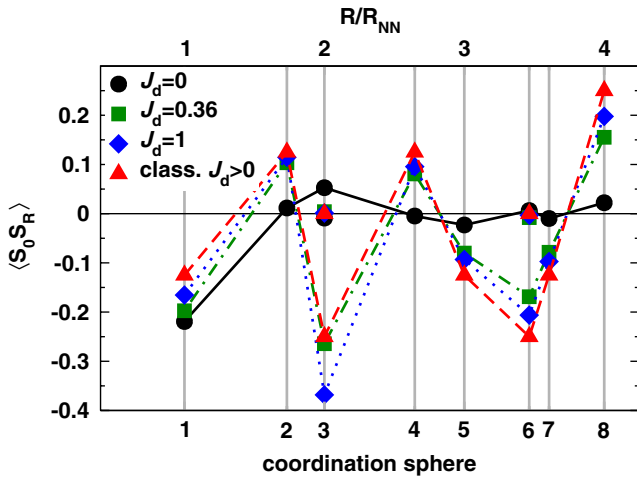FIG. 4 (color online). Exchange integrals of kapellasite and haydeeite as a function of Coulomb repulsion U.

FIG. 5 (color online).   GS spin-spin correlation $\langle \mathbf{S_0 S_R} \rangle$ versus separation $R = |\mathbf{R}|$ for the $J_1 - J_d$ HAFM on the kagome lattice. The results for the quantum $S = 1/2$ model are calculated for a finite lattice of $N = 36$ sites. The lines are guides for the eyes connecting data points. Note that for $R = 2$ and $\sqrt{12}$, two nonequivalent spin-spin separations exist and the lines connect the points representing the stronger correlation.

tions [11,12] leading to different low-temperature behavior of the specific heat C (power-law in T) and the susceptibility χ (exponential decay). By contrast, we find that for $\alpha = 1$ ($\alpha = 0.36$) there are no (only a few) singlets within the spingap. Therefore, we do not expect any basic difference in the low-T behavior of C and χ.

To summarize, we have performed electronic structure calculations for two new spin-1/2 kagome lattice compounds—kapellasite and haydeeite. Both compounds are 2D magnets, with two relevant AF exchanges: NN exchange J_1 and the exchange along "diagonals" of a kagome lattice J_d. We find $\alpha \equiv J_d/J_1 \approx 0.36$ for kapellasite and $\alpha \approx 1$ for haydeeite. The exchanges and thus α values are strongly dependent on the H position for which the experimental value is unlikely with respect to the total energy and should be reinvestigated. The presence of significant J_d interaction leads to (i) noncoplanar magnetic order with 12 sublattices on the classical level which at least on a short-range scale shows similarities to the quantum model, and (ii) to the shift of the low-lying singlets out of the spingap. We especially emphasize the crucial importance of J_d for all real materials with kagome geometry, which needs careful consideration in order to obtain the physically relevant model for the GS and the low-lying excitations. This work is a starting point for study of these promising model compounds. Our predictions could be challenged and extended by low-temperature experiments: neutron scattering and μSR to probe the spin-spin correlation function, thermodynamic measurements (C and χ, see above) to check for a possible spin gap, including pressure studies to modify α via a change of the O–H distance.

*rosner@cpfs.mpg.de

[1] R. Moessner, Can. J. Phys. **79**, 1283 (2001).
[2] *Frustrated Spin Systems*, edited by H. T. Diep (World Scientific, Singapore, 2004).
[3] *Quantum Magnetism*, edited by U. Schollwoeck *et al.* (Springer, New York, 2004).
[4] R. Moessner and A. P. Ramirez, Phys. Today **59**, No. 2, 24 (2006).
[5] S. Sachdev, Lect. Notes Phys. **645**, 381 (2004).
[6] A. A. Tsirlin *et al.*, Phys. Rev. B **77**, 092402 (2008).
[7] H. Kageyama *et al.*, Phys. Rev. Lett. **82**, 3168 (1999).
[8] J. T. Chalker, P. C. W. Holdsworth, and E. F. Shender, Phys. Rev. Lett. **68**, 855 (1992).
[9] D. A. Huse and A. D. Rutenberg, Phys. Rev. B **45**, 7536 (1992).
[10] J. N. Reimers and A. J. Berlinsky, Phys. Rev. B **48**, 9539 (1993).
[11] C. Waldtmann *et al.*, Eur. Phys. J. B **2**, 501 (1998).
[12] C. Lhuillier, P. Sindzingre, and J.-B. Fouet, Can. J. Phys. **79**, 1525 (2001).
[13] M. Rigol and R. R. P. Singh, Phys. Rev. Lett. **98**, 207204 (2007).
[14] B. G. Levi, Phys. Today **60**, No. 2, 16 (2007).
[15] Y. Ran *et al.*, Phys. Rev. Lett. **98**, 117205 (2007).
[16] R. S. W. Braithwaite *et al.*, Mineral. Mag. **68**, 527 (2004).
[17] M. P. Shores *et al.*, J. Am. Chem. Soc. **127**, 13462 (2005).
[18] P. Mendels *et al.*, Phys. Rev. Lett. **98**, 077204 (2007).
[19] J. S. Helton *et al.*, Phys. Rev. Lett. **98**, 107204 (2007).
[20] M. A. de Vries *et al.*, Phys. Rev. Lett. **100**, 157205 (2008).
[21] W. Krause *et al.*, Mineral. Mag. **70**, 329 (2006).
[22] J. Schlüter and T. Malcherek, Neues Jahrb. Mineral., Abh. **184**, 39 (2007).
[23] K. Koepernik and H. Eschrig, Phys. Rev. B **59**, 1743 (1999).
[24] J. P. Perdew and Y. Wang, Phys. Rev. B **45**, 13244 (1992).
[25] H. Eschrig, K. Koepernik, and I. Chaplygin, J. Solid State Chem. **176**, 482 (2003).
[26] T. Malcherek and J. Schlüter, Acta Crystallogr. Sect. B **63**, 157 (2007).
[27] The crystal structures were determined by x-ray diffraction; this method usually does not allow to define the H position with good precision.
[28] Blue transparent crystals evidence a gap of about 3 eV.
[29] See, e.g., Refs. [6,30,31] and references therein.
[30] M. D. Johannes *et al.*, Phys. Rev. B **74**, 174435 (2006).
[31] O. Janson *et al.*, Phys. Rev. B **76**, 115119 (2007).
[32] $U_{\text{eff}} = 4$ eV was used. Thus, the mapping is well justified in the strongly correlated limit $U_{\text{eff}} \gg t_i$ at half filling.
[33] J.-C. Domenge *et al.*, Phys. Rev. B **72**, 024433 (2005).
[34] The GS's are similar to the GS shown in Fig. 2 in Ref. [33].
[35] O. Starykh, R. Singh, and G. Levine, Phys. Rev. Lett. **88**, 167203 (2002).
[36] R. Coldea *et al.*, Phys. Rev. Lett. **86**, 1335 (2001).